Nonreciprocal photonic surface states in periodic structures of magnetized plasma nanospheres

A. Christofi* and N. Stefanou

Department of Solid State Physics, University of Athens, Panepistimioupolis, GR-157 84 Athens, Greece

(Received 2 July 2013; published 23 September 2013)

We report on the occurrence and properties of photonic surface states in periodic structures of magnetized plasma nanospheres by means of rigorous calculations using the full-electrodynamic layer-multiple-scattering method, properly extended to treat gyrotropic spheres with arbitrarily oriented gyration vector. More specifically, dispersion diagrams of Tamm states at the (001) surface of a semi-infinite fcc crystal of plasma nanospheres and of guided modes of a square array of such spheres supported by a quartz substrate, without and under the action of an in-plane static uniform magnetic field, are analyzed and nonreciprocal optical response, which emerges as a result of the simultaneous lack of space-inversion and time-reversal symmetries, is demonstrated in the Voigt geometry.

DOI: 10.1103/PhysRevB.88.125133 PACS number(s): 42.70.Qs, 41.20.Jb, 42.25.Bs

Excitations at the surface of a plasmonic material (metal or semiconductor), in the presence of a magnetic field, can exhibit nonreciprocal behavior due to the simultaneous lack of space-inversion and time-reversal symmetries.[1,2] Such a nonreciprocal behavior was for instance observed in the reflection of light at the surface of an n-type InSb crystal with respect to field and light-propagation reversal.[3] More recently, the existence of one-way electromagnetic (EM) modes in a planar waveguide formed in the region between a semi-infinite metal and a semi-infinite photonic crystal, under a static uniform magnetic field, was also reported.[4] In a versatile alternative design[5] with a photonic crystal made from a transparent dielectric material that exhibits a strong magneto-optical activity, such as bismuth iron garnet, nonreciprocity was found at relatively weak magnetic fields.

Plasmonic nanostructures can exhibit a substantial magneto-optical activity due to the excitation of localized surface plasmon resonance modes[6] and discontinuous surfaces consisting of plasma nanoparticles provide a more flexible platform for tailoring plasmons by varying the shape and geometrical arrangement of the particles as well as their dielectric environment, compared to the corresponding homogeneous plasma surface.[7–13] However, nonreciprocal effects in the optical response of such discontinuous surfaces under the action of an external magnetic field have not yet been investigated in detail. In the present paper we report a systematic theoretical study of spectral nonreciprocity of surface guided modes localized at the (001) surface of a semi-infinite fcc crystal of plasma nanospheres and at a single (001) layer of this crystal deposited on a substrate.

Our calculations are based on the full-electrodynamic layer-multiple-scattering method that we recently extended to photonic structures of gyrotropic spheres.[14] A detailed description of the method can be found elsewhere.[15,16] Here, we restrict ourselves in saying that we evaluate the scattering T matrix of a gyrotropic sphere in a spherical-wave basis from a set of coupled linear equations that relate the expansion coefficients of the scattered to those of the incident field.[17–20] If the gyration vector is oriented along the z direction, the T matrix has a block diagonal form: $T_{Plm;P'l'm'} = T^{(m)}_{Pl;P'l'}\delta_{mm'}$, where P stands for the polarization mode, magnetic (H) or electric (E), and l,m are the usual angular momentum indices. Moreover, $T^{(m)}_{Pl;P'l'}$ vanishes identically if the magnetic/electric multipoles corresponding to Pl and $P'l'$ do not have the same parity, even or odd, which means that the T matrix in a given m subspace is further reduced into two submatrices. The above symmetry properties, however, do not hold in any coordinate system. In general, if α,β,γ are the Euler angles transforming an arbitrarily chosen coordinate system into the given coordinate system in which the gyration vector is oriented along the z axis, the T matrix is given by

$$T_{Plm;P'l'm'} = \sum_{m''} D^{(l)}_{mm''}(\alpha,\beta,\gamma)T^{(m'')}_{Pl;P'l'}D^{(l')}_{m''m'}(-\gamma,-\beta,-\alpha), \tag{1}$$

where $D^{(l)}$ are the appropriate transformation matrices associated with the l irreducible representation of the $O(3)$ group.[21]

We assume that the plasma nanospheres of the structures under consideration are characterized by a relative magnetic permeability $\mu_p = 1$ and by the simple yet effective Drude relative electric permittivity[22]

$$\epsilon_p = 1 - \frac{\omega_p^2}{\omega^2[1 + i/(\tau\omega)]}, \tag{2}$$

where τ is the relaxation time of the free carriers and ω_p is the bulk plasma frequency: $\omega_p^2 = ne^2/(m\epsilon_0)$, with n, $-e$, and m the carrier density, charge, and mass, respectively, which naturally introduces c/ω_p as the length unit. We note that, assuming $\hbar\omega_p \simeq 10$ eV, which is a typical value for metals, c/ω_p corresponds to about 20 nm. For semiconductors, on the other hand, as their carrier densities can be easily varied within a broad range of values, which are much lower than those in metals, the plasma frequency is much smaller (typically at mid- and far-infrared frequencies) and the length unit c/ω_p increases accordingly.

In the presence of a static uniform magnetic field $\mathbf{B}$, the response of a plasma to a time-harmonic EM wave of angular frequency ω, with electric-field component $\mathbf{E} = \mathbf{E}_0\exp(-i\omega t)$, is described by the equation of motion of the electrons: $m\ddot{\mathbf{r}} = -m\tau^{-1}\dot{\mathbf{r}} - e\mathbf{E} - e\dot{\mathbf{r}}\times\mathbf{B}$. The resulting polarization density, $\mathbf{P} = -ne\mathbf{r}$, defines an electric displacement vector $\mathbf{D} = \epsilon_0\mathbf{E} + \mathbf{P}$ and finally yields the relative electric permittivity tensor $\overleftrightarrow{\epsilon_g}$ of the magnetized plasma through

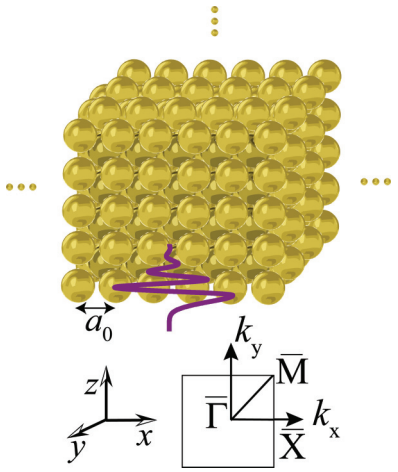

FIG. 1. (Color online) A semi-infinite fcc crystal of Drude spheres (nearest neighbor distance: $a_0 = 2.2c/\omega_p$; sphere radius: $S = c/\omega_p$), grown along its [001] direction, with a surface state (schematic representation) and the corresponding surface Brillouin zone.

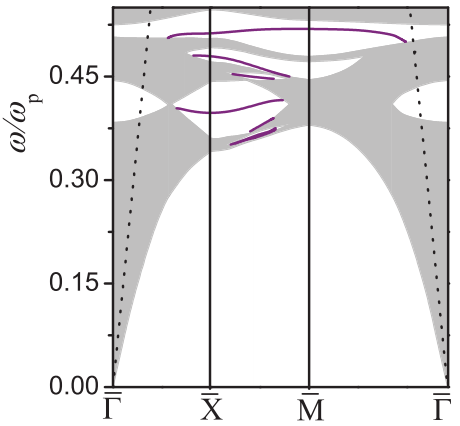

FIG. 2. (Color online) Projection of the photonic band structure of the crystal of Fig. 1 on symmetry lines of its (001) surface Brillouin zone. Shaded and blank regions represent frequency bands and gaps, respectively. With solid lines in gap regions we show the dispersion curves of the surface modes. The dotted lines denote the light cone in the host medium (air).

$\mathbf{D} = \epsilon_0 \overleftrightarrow{\epsilon_g} \mathbf{E}$. Defining the cyclotron resonance frequency, $\omega_c = eB/m$, if $\mathbf{B}$ is oriented along the z direction, after some straightforward algebra we find that $\overleftrightarrow{\epsilon_g}$ has the gyrotropic form

$$\overleftrightarrow{\epsilon_g} = \begin{pmatrix} 1 - \dfrac{\omega_p^2 \xi}{\omega^2 \xi^2 - \omega_c^2} & i\dfrac{\omega_c}{\omega}\dfrac{\omega_p^2}{\omega^2 \xi^2 - \omega_c^2} & 0 \\ -i\dfrac{\omega_c}{\omega}\dfrac{\omega_p^2}{\omega^2 \xi^2 - \omega_c^2} & 1 - \dfrac{\omega_p^2 \xi}{\omega^2 \xi^2 - \omega_c^2} & 0 \\ 0 & 0 & 1 - \dfrac{\omega_p^2}{\omega^2 \xi^2} \end{pmatrix}, \tag{3}$$

with $\xi = 1 + i/(\tau\omega)$. We note that, by setting $\omega_c = 0$, $\overleftrightarrow{\epsilon_g}$ becomes a diagonal tensor with all of its diagonal elements equal to ϵ_p given by Eq. (2), as expected. In our calculations we shall neglect dissipative losses ($\tau^{-1} = 0$) in order to ensure an unambiguous interpretation of the photonic dispersion diagrams.

We first consider a semi-infinite fcc crystal of plasma spheres, grown along its [001] direction, as shown in Fig. 1. The spheres have a radius $S = c/\omega_p$ and the nearest neighbor distance in the fcc lattice is $a_0 = 2.2c/\omega_p$. It has been recently shown that this crystal supports surface, so-called Tamm, states at its (001) surface.[23] The dispersion curve $\omega(\mathbf{k}_\parallel)$, where $\mathbf{k}_\parallel$ is the in-plane (x-y) wave vector component reduced within the surface Brillouin zone of an optical Tamm state, lies outside the light cone in the host medium and at the same time within a frequency gap of the crystal. This ensures that the associated EM field decreases exponentially on either side of the surface. Moreover, the dispersion of a surface state satisfies the reciprocity condition $\omega(-\mathbf{k}_\parallel) = \omega(\mathbf{k}_\parallel)$. In Fig. 2 we display the projection of the photonic band structure of the crystal of Fig. 1 on symmetry lines of its (001) surface Brillouin zone. The shaded regions represent frequency bands, i.e., at any frequency within a shaded region, for given $\mathbf{k}_\parallel$, there exists at least one propagating EM mode in the infinite crystal. The blank regions represent frequency gaps for the given $\mathbf{k}_\parallel$. With solid lines in the gap regions we show the dispersion of surface states, while the dotted straight lines denote the light cone in the air host. These modes lie indeed in gap regions and outside the light cone, i.e., they are true surface states that decay exponentially in the crystal as well as in the outer region.

The formation of frequency bands and gaps outside the air light cone as well as of the Tamm states of Fig. 2 can be understood by considering corresponding finite slabs with progressively increasing thickness. In Fig. 3 we present the dispersion diagrams of the eigenmodes of one-, two-, and four-layers thick (001) slabs of the crystal of Fig. 1, along $\overline{\Gamma X}$. The wave field associated with these eigenmodes is localized within the given slab and decays exponentially in the outer region. It can be seen from Fig. 3 that, as the number of layers increases, the band regions of the infinite crystal outside the air light cone are progressively filled with slab modes while the gap regions remain empty. Moreover, for a multilayer slab, we obtain two

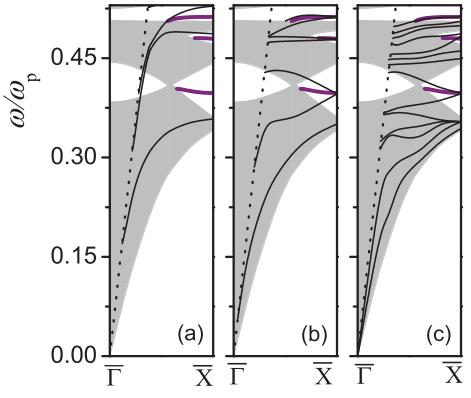

FIG. 3. (Color online) Formation of the band and gap regions outside the light cone in the air host, as well as of the surface states, of Fig. 2 from the slab modes of (a) one-, (b) two-, and (c) four-layers thick (001) slabs of the crystal of Fig. 1, along $\overline{\Gamma X}$.

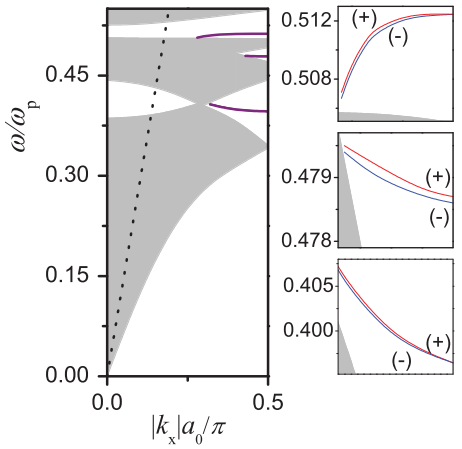

FIG. 4. (Color online) Influence of a static uniform magnetic field corresponding to $\omega_c = 0.01\omega_p$ applied along the [110] direction of the fcc crystal of Fig. 1, which is taken to be the y axis, on the dispersion curves of the surface states of Fig. 2 in the k_x direction. An enlarged view of these dispersion curves is displayed in the right-hand panel, with the (+) and (−) signs denoting positive and negative values of k_x, respectively.

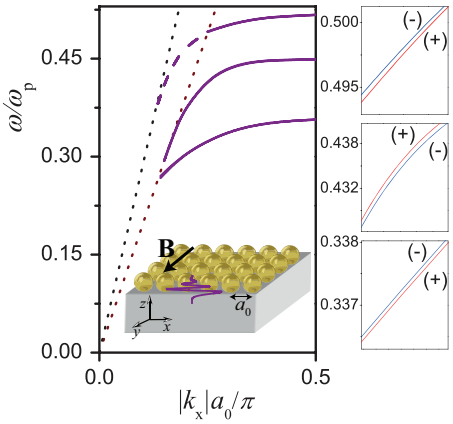

FIG. 5. (Color online) Dispersion diagram in the k_x direction of the guided modes of a square array of Drude spheres (lattice constant: $a_0 = 2.2c/\omega_p$; sphere radius: $S = c/\omega_p$) on a quartz substrate, under the action of a static uniform magnetic field corresponding to $\omega_c = 0.01\omega_p$ applied in the y direction (see inset). The dotted lines denote the light cones in air and quartz. An enlarged view of the dispersion curves of these modes is displayed in the right-hand panel, with the (+) and (−) signs denoting positive and negative values of k_x, respectively.

additional dispersion curves, close to each other in frequency, which correspond to modes localized at the two surfaces of the slab, as shown in Figs. 3(b) and 3(c). As the number of layers in the slab increases, interaction between these modes becomes weaker and their dispersion curves converge to those of the corresponding Tamm states of the semi-infinite crystal of Fig. 3.

In Fig. 4 we display the dispersion diagram of the Tamm states of Fig. 2 along $\overline{\Gamma X}$ under the influence of an external static uniform magnetic field, applied parallel to the surface, along the y direction, corresponding to $\omega_c = 0.01\omega_p$. This value of ω_c, though it is by an order of magnitude smaller than that considered by Yu *et al.*,[4] for metals corresponds to a prohibitively strong magnetic field, of the order of 10^3 T, but for semiconductors the field becomes much weaker, of the order of 1 T or less. Since in this case the static magnetic field is not oriented along the z direction, which is by definition the direction of growth of the crystal in the layer-multiple-scattering method, the calculations involved require transforming the T matrix according to Eq. (1) using the appropriate Euler angles: $\alpha = 90^\circ, \beta = 90^\circ, \gamma = 0^\circ$.[24] As we can see from the enlarged view of the dispersion curves, the propagation of the surface states along the direction normal to the magnetic field changes and becomes nonreciprocal: $\omega(-k_x) \neq \omega(k_x)$. Reversal of the magnetic field direction has the same effect as reversal of the propagation direction ($k_x \rightarrow -k_x$) while, if the magnetic field is perpendicular to the surface or parallel to the propagation direction, nonreciprocity is not encountered. As a result of the spectral splitting of the dispersion curves associated with the forward and backward propagating waves, within a short frequency range near their band edges, only modes propagating in one direction exist, as shown in Fig. 4. The relative spectral shift of the bands depends on the magnitude of the external field, which allows for the design of tunable surface states for one-way light transport. A similar nonreciprocal behavior has been reported for surface modes at truncated one-dimensional magnetophotonic crystals.[25] It should be noted that nonreciprocity also occurs in surface resonant states that lie inside the light cone in the host medium and thus can be excited by an incident EM wave. Excitation of such waves was recently shown to lead to the phenomenon of one-way extraordinary optical transmission through a perforated metal film in a magneto-optical environment, at oblique incidence.[26] Such leaky surface modes which, lying within a band gap, would of course not be transmitted through the crystal, do not appear in our case.

From Fig. 3(a) it is clear that even a single (001) layer of the crystal of Fig. 1 supports guided modes of the EM field, localized in the monolayer. However, in this case, application of a static uniform magnetic field cannot render these modes nonreciprocal because of the existence of space-inversion symmetry. This symmetry can be broken if the layer is deposited on a substrate. In Fig. 5, we display the dispersion diagram along k_x of the guided modes of this layer on a supporting quartz substrate under the action of a static uniform magnetic field, corresponding to $\omega_c = 0.01\omega_p$, applied along the y direction (see inset to Fig. 5). Again, as can be seen from an enlarged view of the dispersion curves, the propagation of the guided modes along the direction normal to the magnetic field becomes nonreciprocal: $\omega(-k_x) \neq \omega(k_x)$.

It is worth noting that the planar geometries studied in the present work are invariant under the C_{4v} point symmetry group.[21] If an external magnetic field is applied along the z direction, i.e., perpendicular to the surface, the point group is reduced to C_4 since $\mathbf{P}\overleftrightarrow{\epsilon}_g\mathbf{P}^{-1} = \overleftrightarrow{\epsilon}_g$ only for those operations $\widehat{\mathbf{P}}$ of C_{4v} that belong to C_4, and spectral reciprocity $\omega(-\mathbf{k}_\parallel) = \omega(\mathbf{k}_\parallel)$ is always ensured by a rotation through an angle π about the z axis, which is a symmetry operation of C_4. If now the magnetic field is in-plane, say along the y direction, the relevant point symmetry group C_{1h} consists of the identity and reflection with respect to the x-z plane operations.[21] Therefore, while reciprocity along the y direction, $\omega(-k_y) = \omega(k_y)$, is ensured by mirror symmetry

with respect to the x-z plane, $\omega(-k_x) \neq \omega(k_x)$ because there is no group symmetry operation which transforms $(k_x,0,0)$ into $(-k_x,0,0)$, given also the lack of time-reversal symmetry. Therefore, in the structures under study, nonreciprocity occurs in the Voigt (Cotton-Mouton) geometry, for an in-plane external magnetic field.

In concluding this paper, it should be noted that magneto-optic effects, being proportional to the magnitude of the nondiagonal elements of $\overleftrightarrow{\epsilon_g}$, are expected to increase (cubically in the $\omega_c \ll \omega < \omega_p$ regime) with ω_p/ω. Therefore, stronger spectral nonreciprocity is anticipated in corresponding structures of magnetized plasma nanoshells with optimized geometric parameters[23] or/and dielectric environment. It is also worth noting that the effects discussed in this paper can also occur in corresponding structures of magnetic garnet spheres, which exhibit a quite strong gyrotropic response in moderate magnetic fields.

A.C. is supported by a SPIE Optics and Photonics Education Scholarship.

*aristi@ims.demokritos.gr

[1] I. Vitebsky, J. Edelkind, E. N. Bogachek, A. G. Scherbakov, and U. Landman, Phys. Rev. B **55**, 12566 (1997).
[2] A. Figotin and I. Vitebsky, Phys. Rev. E **63**, 066609 (2001).
[3] L. Remer, E. Mohler, W. Grill, and B. Lüthi, Phys. Rev. B **30**, 3277 (1984).
[4] Z. Yu, G. Veronis, Z. Wang, and S. Fan, Phys. Rev. Lett. **100**, 023902 (2008).
[5] V. Kuzmiak, S. Eyderman, and M. Vanwolleghem, Phys. Rev. B **86**, 045403 (2012).
[6] B. Sepúlveda, J. B. González-Díaz, A. García-Martín, L. M. Lechuga, and G. Armelles, Phys. Rev. Lett. **104**, 147401 (2010).
[7] N. Félidj, J. Aubard, G. Lévi, J. R. Krenn, G. Schider, A. Leitner, and F. R. Aussenegg, Phys. Rev. B **66**, 245407 (2002).
[8] J. Aizpurua, P. Hanarp, D. S. Sutherland, M. Käll, G. W. Bryant, and F. J. García de Abajo, Phys. Rev. Lett. **90**, 057401 (2003).
[9] P. Hanarp, M. Käll, and D. S. Sutherland, J. Phys. Chem. B **107**, 5768 (2003).
[10] N. Papanikolaou, Phys. Rev. B **75**, 235426 (2007).
[11] G. Gantzounis, N. Stefanou, and N. Papanikolaou, Phys. Rev. B **77**, 035101 (2008).
[12] C. Tserkezis, N. Papanikolaou, E. Almpanis, and N. Stefanou, Phys. Rev. B **80**, 125124 (2009).
[13] C. Y. Tsai, K. H. Chang, C. Y. Wu, and P. T. Lee, Opt. Express **21**, 14090 (2013).
[14] A. Christofi and N. Stefanou, Phys. Rev. B **87**, 115125 (2013).
[15] N. Stefanou, V. Yannopapas, and A. Modinos, Comput. Phys. Commun. **113**, 49 (1998).
[16] N. Stefanou, V. Yannopapas, and A. Modinos, Comput. Phys. Commun. **132**, 189 (2000).
[17] G. W. Ford and S. A. Werner, Phys. Rev. B **18**, 6752 (1978).
[18] Z. Lin and S. T. Chui, Phys. Rev. E **69**, 056614 (2004).
[19] J. L. W. Li and W. L. Ong, IEEE Trans. Antennas Propag. **59**, 3370 (2011).
[20] J. L.-W. Li, W.-L. Ong, and K. H. R. Zheng, Phys. Rev. E **85**, 036601 (2012).
[21] T. Inui, Y. Tanabe, and Y. Onodera, *Group Theory and its Applications in Physics* (Springer, Berlin, 1990).
[22] N. W. Ashcroft and N. D. Mermin, *Solid State Physics* (Saunders, New York, 1976).
[23] C. Tserkezis, N. Stefanou, G. Gantzounis, and N. Papanikolaou, Phys. Rev. B **84**, 115455 (2011).
[24] M. I. Mishchenko, L. D. Travis, and A. A. Lacis, *Scattering, Absorption, and Emission of Light by Small Particles* (Cambridge University Press, Cambridge, UK, 2002).
[25] A. B. Khanikaev, A. V. Baryshev, M. Inoue, and Y. S. Kivshar, Appl. Phys. Lett. **95**, 011101 (2009).
[26] A. B. Khanikaev, S. H. Mousavi, G. Shvets, and Y. S. Kivshar, Phys. Rev. Lett. **105**, 126804 (2010).